Cell Reports, Volume *22*

Supplemental Information

Pharmacological Inhibition of Necroptosis Protects from Dopaminergic Neuronal Cell Death in Parkinson's Disease Models

Angelo Iannielli, Simone Bido, Lucrezia Folladori, Alice Segnali, Cinzia Cancellieri, Alessandra Maresca, Luca Massimino, Alicia Rubio, Giuseppe Morabito, Leonardo Caporali, Francesca Tagliavini, Olimpia Musumeci, Giuliana Gregato, Erwan Bezard, Valerio Carelli, Valeria Tiranti, and Vania Broccoli

Supplemental Procedures

In vitro neuronal differentiation of iPSCs

NPCs were generated as previously described with appropriated optimization (Marchetto et al., 2010). Briefly, iPSCs were dissociated in cell clusters using Accutase (Sigma-Aldrich) and seeded onto low-adhesion plates in mTeSR1 supplemented with N2 (1:200, ThermoFisher Scientific), Pen/Strept (1%, Sigma-Aldrich), human Noggin (0.5 μg/ml, R&D System), SB431542 (5 μM, Sigma-Aldrich) and Y27632 (10 μM, Milteny Biotec). After 10 days, embryoid bodies were seeded onto matrigel-coated plates (1:100, matrigel growth factor reduced, Corning) in DMEM/F12 (Sigma-Aldrich) supplemented with N2 (1:100), non-essential amino acids (1%, MEM NEAA, ThermoFisher Scientific) and Pen/Strept. After 10 days, rosettes were dissociated with Accutase and plated onto matrigel coated-flasks in NPC media containing DMEM/F12, N2 (1:200), B27 (1:100, ThermoFisher Scientific), Pen/Strept (1%) and FGF2 (20 ng/ml, ThermoFisher Scientific).
For differentiation, NPCs were dissociated with Accutase and plated on matrigel-coated 24-well plates (1× 20000 cells per well) in NPC medium. Two days after, the differentiation medium containing Neurobasal (ThermoFisher Scientific), Pen/Strep (1%), B27 (1:50), Sonic Hedgehog (50 ng/ml, Sigma-Aldrich) and CHIR99021 (0,8 μM, Stemgent) was added and kept for 11 days. During this period half medium was replaced every 2-3 days. After 11 days the differentiation medium was replaced with Neurobasal, Pen/Strep (1%), B27 (1:50), human BDNF (10 ng/ml, PeproTech), human GDNF (10 ng/ml, PeproTech), Forskolin (10 μM, Sigma-Aldrich), Ascorbic Acid (20 μM, Sigma-Aldrich) and Purmorphamine (200 nM, Stemgent) for terminal differentiation. At this stage half of the medium was changed every 2–3 days.

RNA isolation and real-time RT-PCR

RNA was extracted using the TRI Reagent isolation system (Sigma-Aldrich) according to the manufacturer's instructions. Total RNA was treated with DNAseI (Roche) to prevent DNA contamination. One microgram of RNA was reverse transcribed using the iScript Reverse Transcription Supermix for RT-qPCR (Bio-Rad, USA). Quantitative RT-PCR (qRT-PCR) was carried out using the CFX96 Real-Time PCR Detection System (Bio-Rad, USA). One-fiftieth of the reverse-transcribed cDNA was amplified in a 16μl reaction mixture containing 1× Titan Hot Taq EvaGreen qPCR Mix (Bioatlas, Estonia) and 0.4 mM of each primer. The thermal profile consisted of 2 minutes at 50°C and 10 minutes at 95°C, followed by 40 cycles of 15 seconds each at 95°C and 1 minute at 60°C. mRNA levels were calculated according to the threshold cycle numbers within a linear range of amplification of 20 to 32 cycles. Data were standardized versus the housekeeping

gene Actin, which was used as an internal standard and amplified for every sample in parallel assays.

Mitotracker Green and Orange

NPCs from patients and controls were incubated with 50 nM of Mitotracker Green and Mitotracker Orange (Molecular Probes) for 30 min at 37 °C, washed with PBS and acquired by confocal microscope (Leica TCS SP5, Germany). For the analysis, the samples were acquired on LSR-Fortessa (BD) flow cytometer. All data were analyzed using FCS Ex4press 6 Flow (De Novo Software) and expressed as mean fluorescence intensity.

Lysotracker Red

NPCs from patients and controls were incubated with 50 nM of Lysotracker Red (Molecular Probes) for 30 min at 37 °C, washed with PBS and acquired by confocal microscope (Leica TCS SP5, Germany). The quantification of the signal was performed using ImageJ software (NIH, USA).

Mitochondrial Morphology

NPCs from patients and controls were dissociated with Accutase and plated on matrigel-coated 24-well plates (1x40000 cells per well) in NPC medium. Mitochondrial morphology was assessed by TOMM20 immunostaining. Cellular fluorescence images were acquired with a Nikon Eclipse Ni microscope. Images were collected using a X63/1.4 oil objective and analyzed using Mito-Morphology macro in ImageJ.

Micro-oxygraphy assays

The day before analysis, NPCs from patients and normal donors were dissociated with Accutase and plated at a density of 20.000 cells per well in a Polyornithine-Laminin coated 96-well multiwell plate and incubated over night at 37°C with 5% CO_2. After 24 hours, 25mM glucose was added in the medium to perform the subsequent analysis. Drugs were added sequentially to the cells in the following order: Oligomycin 1 μM (Sigma-Aldrich), FCCP (Carbonyl cyanide 4-(trifluoromethoxy)phenylhydrazone) 2,1 μM (Sigma-Aldrich) and Rotenone 0,5 μM (Sigma-Aldrich). Measurements were done with Seahorse XFe96 Analyzer (Agilent, USA) and normalized on cell counts, calculated with CyQuant Direct Cell Proliferation Assay Kit (Life Technologies).

Mitochondrial DNA sequencing and quantification

Total DNA from cells was extracted using the NucleoSpin Tissue kit (Machery & Nagel), following manufacturer's instructions. The entire mtDNA molecule was sequenced by NGS approach. First, mtDNA was amplified in two long PCR amplicons (9.1 kb and 11.2 kb) using Q5 High-Fidelity DNA Polymerase (New England Biolabs, UK) and purified by Agencourt AMPure XP (Beckman Coulter Life Sciences, Italy). Subsequently, the library was constructed by Nextera XT DNA Library Preparation Kit (Illumina, San Diego, CA) and sequenced on MiSeq System (Illumina, San Diego, CA), using the 600-cycle reagent kit. All changes are relative to the revised Cambridge Reference Sequence (rCRS, NC_012920). Quantitative Real Time PCR was used to assess mtDNA content *per* cell, using a previously described method (Mussini et al., 2005).

RNA sequencing and bioinformatics analysis

Total RNA isolation was performed with RNeasy Mini Kit (QIAGEN). RNA libraries were generated starting from 1 μg of total RNA extracted using TRIzol (Invitrogen, Life Technologies). RNA quality was assessed by using a Tape Station instrument (Agilent). To avoid over-representation of 3'ends, only high-quality RNA with RNA Integrity Number (RIN) ≥ 8 was used. RNA was processed according to the TruSeq Stranded mRNA Library Prep Kit protocol. The libraries were sequenced on an Illumina HiSeq 3000 with 150bp paired-end reads using Illumina TruSeq technology. Image processing and basecall were performed using the Illumina Real Time Analysis Software. Fastq files were aligned to the human genome (GRCh38/hg38) by using STAR (Dobin, 2013), a splice junction mapper for RNA-Seq data, together with the corresponding splice junctions Ensembl GTF annotation, using default parameters.

Immunostaining

Cells were seeded on matrigel-coated glass coverslips and they were fixed for 20 min in ice in 4% paraformaldehyde (PFA, Sigma), solution in phosphate-buffered saline (PBS, Euroclone). Then, cells were permeabilized for 30 min in blocking solution, containing 0.5% Triton X-100 (Sigma-Aldrich) and 10% donkey serum (Sigma-Aldrich), and incubated overnight at 4 °C with the primary antibodies in blocking solution. Then, cells were washed with PBS and incubated for 1 h at room temperature with Hoechst and with secondary antibodies. Brain slices were differently processed. Briefly, free-floating 50 μm-thick slices were rinsed in PBS and treated for one hour with a blocking solution containing BSA 3% and Triton X 100 0.3% in PBS. After being blocked, the tissue was incubated with the primary antibody diluted with a solution containing BSA 1%, Triton X100 0.3% over night at room temperature. The slices were then incubated with the secondary antibody. The following antibodies were used: anti-OCT4 (1:100, Abcam), anti-SOX2 (1:300, R&D

Systems), anti-NANOG (1:100, Abcam), anti-TRA1-60 (1:100, Millipore), anti-PAX6 (1:300 Biolegend), anti-NESTIN (1:300 Millipore), anti-TH (1:200 and 1:1000 for cells and slices respectively, Immunological Sciences), anti-MAP2 (1:500, Immunological Sciences), anti-TOMM20 (1:300, Novus), anti-LAMP1 (1:500, Abcam), anti-HNE (1:200, Alpha Diagnostic), anti-AADC (1:100, Novus Biologicals) and anti-VMAT2 (1:200, Millipore). All the secondary antibodies used for the immunofluorescence staining are Alexa Fluor™. For HRP immunohistochemistry labeling, the Dako Envision Polymer™ conjugated with secondary antibody was used.

Striatal TH quantification

Images were taken with Leica DM4000B at 2.5X magnification and analyzed with Image J (NIH, USA). The striatum boundaries were traced and optical density measured in terms of grey levels for 8-bit images.

4-hydroxynonenal staining and quantification

TH and 4-HNE immunostainings were performed as previously described. Single layer pictures were captured using confocal microscope (TCS SP5, Leica, Germany) at 40X magnification. We used a fixed laser power for all the images. 8-bit pictures were then analyzed with Image J software measuring the level of grays of 4-HNE.

Supplemental References

Marchetto, M.C.N., Carromeu, C., Acab, A., Yu, D., Yeo, G.W., Mu, Y., Chen, G., Gage, F.H., and Muotri, A.R. (2010). A Model for Neural Development and Treatment of Rett Syndrome Using Human Induced Pluripotent Stem Cells. Cell *143*, 527–539.

Mussini, C., Pinti, M., Bugarini, R., Borghi, V., Nasi, M., Nemes, E., Troiano, L., Guaraldi, G., Bedini, A., Sabin, C., et al. (2005). Effect of treatment interruption monitored by CD4 cell count on mitochondrial DNA content in HIV-infected patients: a prospective study. Aids *19*, 1627–1633.

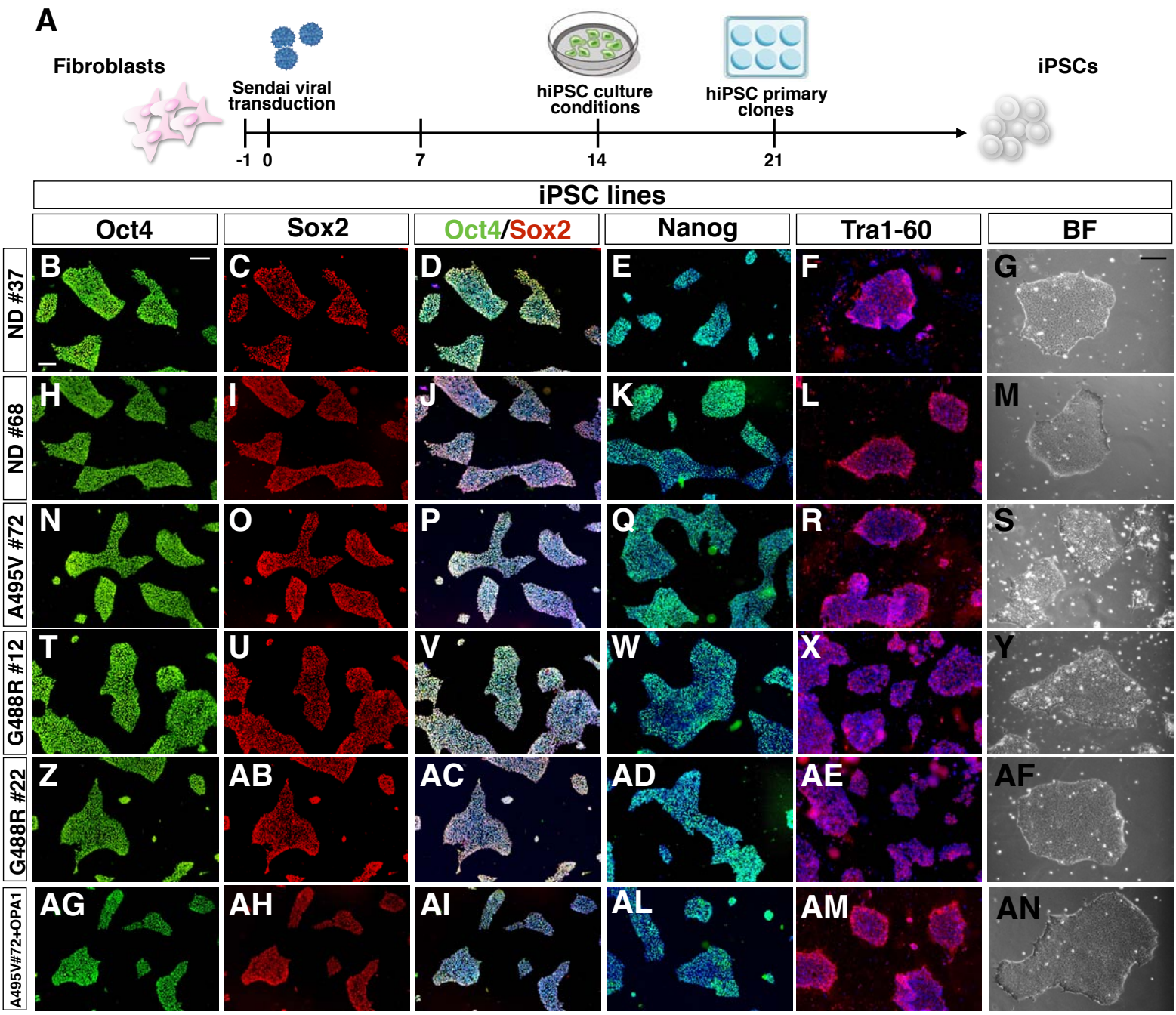
A
Fibroblasts
Sendai viral transduction
hiPSC culture conditions
hiPSC primary clones
iPSCs
-1
0
7
14
21
iPSC lines
Oct4
Sox2
Oct4/Sox2
Nanog
Tra1-60
BF
ND #37
ND #68
A495V #72
G488R #12
G488R #22
A495V#72+OPA1
B
C
D
E
F
G
H
I
J
K
L
M
N
O
P
Q
R
S
T
U
V
W
X
Y
Z
AB
AC
AD
AE
AF
AG
AH
AI
AL
AM
AN

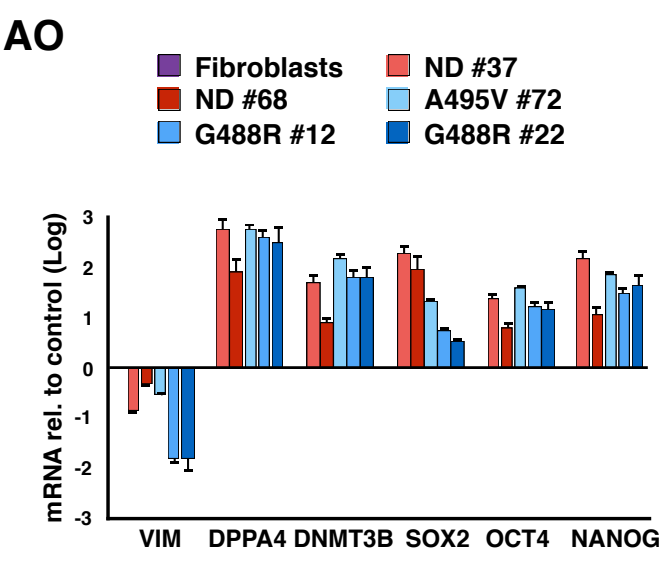
AO
Fibroblasts
ND #68
G488R #12
ND #37
A495V #72
G488R #22
mRNA rel. to control (Log)
3
2
1
0
-1
-2
-3
VIM
DPPA4
DNMT3B
SOX2
OCT4
NANOG

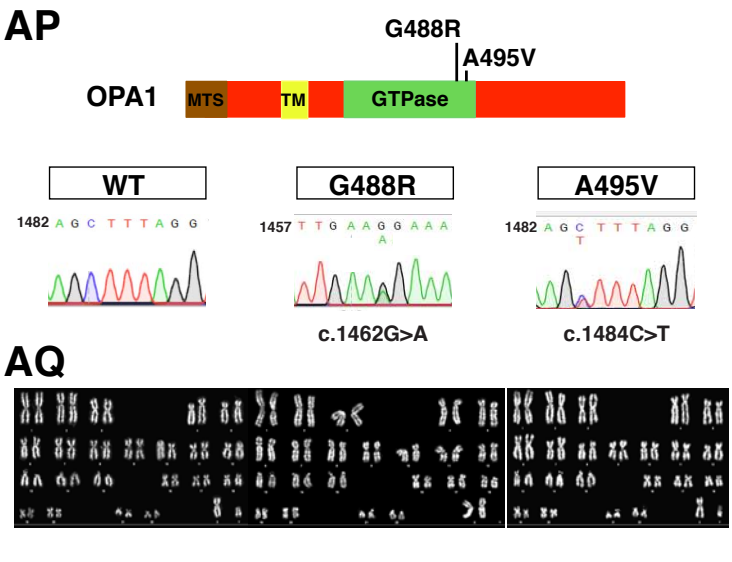
AP
G488R
A495V
OPA1
MTS
TM
GTPase
WT
G488R
A495V
1482 A G C T T T A G G
1457 T T G A A G G A A A
A
1482 A G C T T T A G G
T
c.1462G>A
c.1484C>T
AQ

Figure S1, related to Figure 1.

Development and characterization of PD-OPA1, ND and OPA1-complemented iPSCs.

(**A**) Schematic representation of the protocol for generating iPSCs and (**B-AN**) iPSC colonies immunostained with the pluripotency markers Oct4, Sox2, NANOG and Tra-1-60 and their morphology appearance. (**AO**) qPCR analysis of pluripotency genes in iPSCs compared to the corresponding human fibroblasts. (AP) DNA sequence analysis of the iPSC clones confirming the presence of the two missense heterozygous mutations in OPA1. (**AQ**) Karyotype analysis of iPSC lines displayed a normal euploid chromosome content. Values are mean ± SEM of n=3 independent experiments. Scale bars, 100 μm

A

NT	Gene		Mitomap	ND #37	ND #68	PolyPhen2
7798 C>T	CO2	Syn	Never reported	100	100	-
11511 A>G	ND4	N251S	Never reported	31	-	-
12371 T>C	ND5	L12P	Never reported	26	-	-

NT	Gene		Mitomap	A495V #72	PolyPhen2
7894 A>G	CO2	Syn	16	100	-
11314 A>G	ND4	Syn	63	100	-
12926 A>G	ND5	D197G	-	-	-
16390 G>A	HV1	-	14	-	-

NT	Gene		Mitomap	G488R #12	G488R #22	PolyPhen2
3511A>G	ND1	T69A	Never reported	100	100	-
4853G>C	ND2	Syn	Never reported	58	-	-
13260T>C	ND5	Syn	Never reported	29	49	-
13889G>A	ND5	C516Y	Never reported	100	100	-
15682A>G	CYB	Syn	Never reported	100	12	-
16355C>T	HV1	Syn	Never reported	23	-	-

B

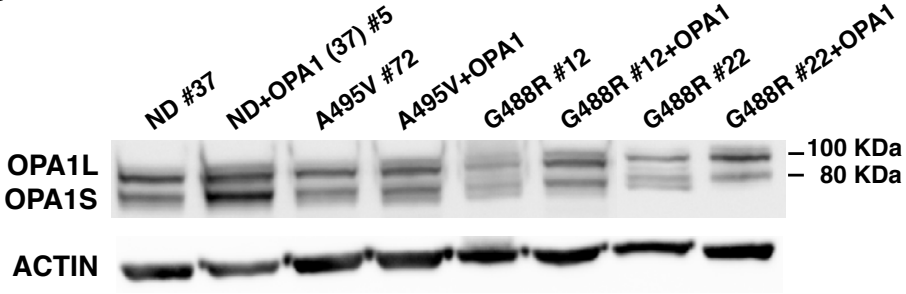

C

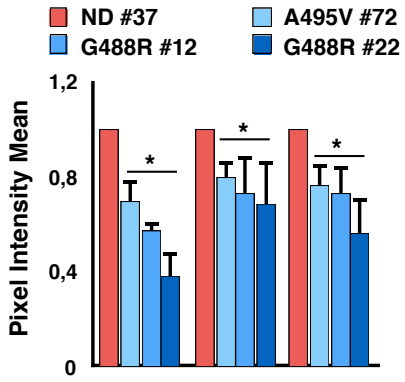

D

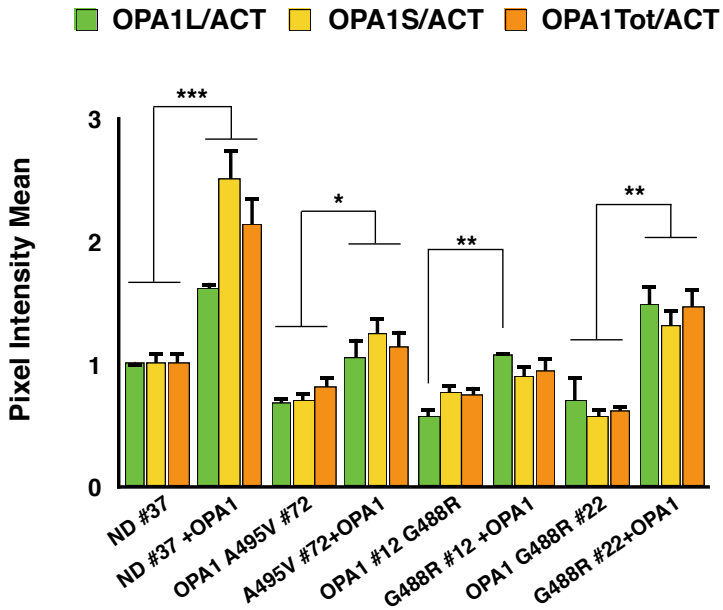

E

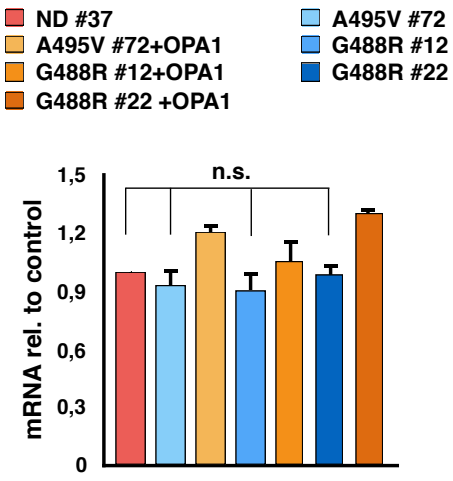

Figure S2, related to Figure 1.

PD-OPA1 iPSCs show reduced OPA1 protein levels.

(**A**) Summary table of the mtDNA sequencing analysis in PD-OPA1 and normal donor iPSC lines. Only private mutations are indicated, with heteroplasmy levels (%), Mitomap frequency and Polyphen2 prediction. Variants defining the haplogroups (H4a1a, H1aq, and H respectively) are not shown. (**B**) Immunoblot analysis for the OPA1 protein in PD-OPA1, ND and OPA1 gene reconstituted iPSCs. (**C**) Quantification of OPA1 protein levels after normalization to the housekeeping protein ACTIN reveals a significant reduction in OPA1 levels in patient compared to ND iPSCs. (**D**) Relative fold change levels of the long (L) and short (S) OPA1 protein forms in PD-OPA1 and relative complemented iPSC lines with respect to the ND #37 iPSC line. (E) qRT-PCR analysis reveals no significant difference in OPA1 transcriptional levels between the different OPA1 genotypes. Data are mean ± SEM of n=3 independent experiments. *P<0,05; **P<0,01; ***P<0,001. Statistical analysis is performed using one-way ANOVA followed by Tukey post- test.

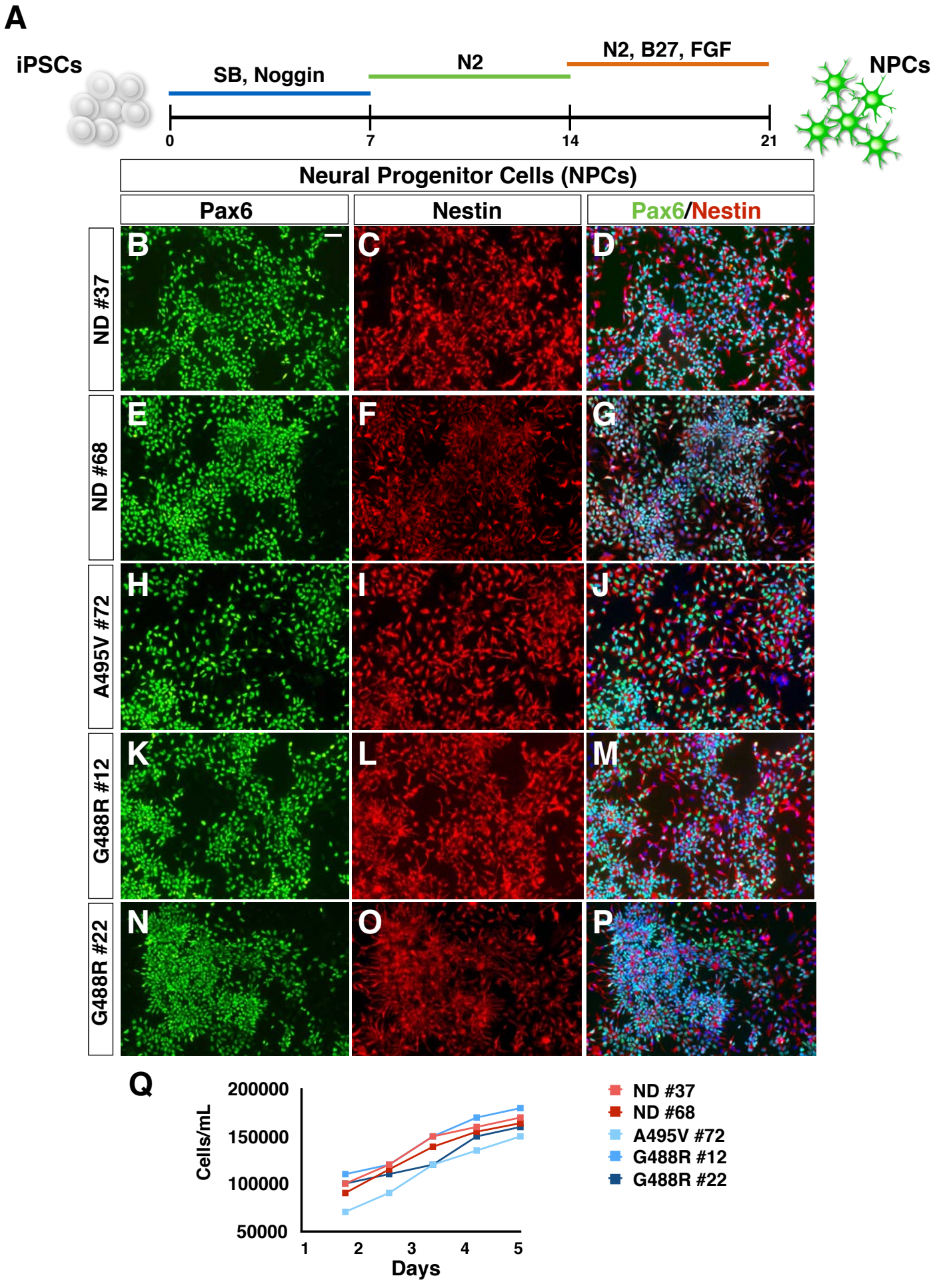
A
iPSCs
SB, Noggin
N2
N2, B27, FGF
NPCs
0
7
14
21
Neural Progenitor Cells (NPCs)
Pax6
Nestin
Pax6/Nestin
ND #37
ND #68
A495V #72
G488R #12
G488R #22
B
C
D
E
F
G
H
I
J
K
L
M
N
O
P
Q
Cells/mL
200000
150000
100000
50000
1
2
3
4
5
Days
ND #37
ND #68
A495V #72
G488R #12
G488R #22

Figure S3, related to Figure 1.

Generation of NPCs.

(**A**) Schematic representation of the procedure for generating NPCs. (**B-P**) Pax6 (green) and Nestin (red) immunofluorescence staining of PD-OPA1 and ND NPCs. (**Q**) Cell growth curve analysis shows a comparable proliferation rate in all the NPC populations irrespective of their genotype. Scale bars, 100 μm.

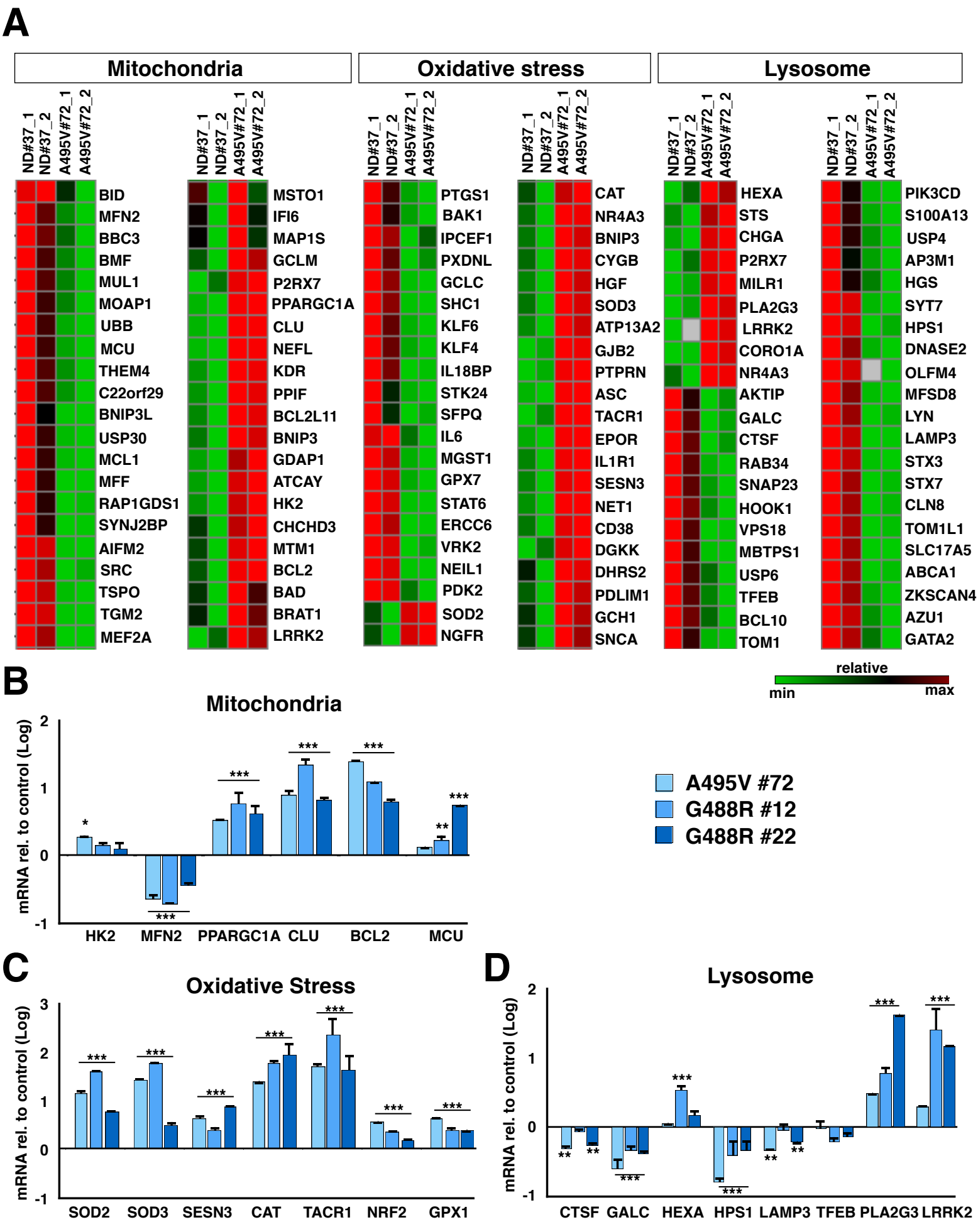
A
Mitochondria
Oxidative stress
Lysosome
ND#37_1
ND#37_2
A495V#72_1
A495V#72_2
BID
MFN2
BBC3
BMF
MUL1
MOAP1
UBB
MCU
THEM4
C22orf29
BNIP3L
USP30
MCL1
MFF
RAP1GDS1
SYNJ2BP
AIFM2
SRC
TSPO
TGM2
MEF2A
MSTO1
IFI6
MAP1S
GCLM
P2RX7
PPARGC1A
CLU
NEFL
KDR
PPIF
BCL2L11
BNIP3
GDAP1
ATCAY
HK2
CHCHD3
MTM1
BCL2
BAD
BRAT1
LRRK2
PTGS1
BAK1
IPCEF1
PXDNL
GCLC
SHC1
KLF6
KLF4
IL18BP
STK24
SFPQ
IL6
MGST1
GPX7
STAT6
ERCC6
VRK2
NEIL1
PDK2
SOD2
NGFR
CAT
NR4A3
BNIP3
CYGB
HGF
SOD3
ATP13A2
GJB2
PTPRN
ASC
TACR1
EPOR
IL1R1
SESN3
NET1
CD38
DGKK
DHRS2
PDLIM1
GCH1
SNCA
HEXA
STS
CHGA
P2RX7
MILR1
PLA2G3
LRRK2
CORO1A
NR4A3
AKTIP
GALC
CTSF
RAB34
SNAP23
HOOK1
VPS18
MBTPS1
USP6
TFEB
BCL10
TOM1
PIK3CD
S100A13
USP4
AP3M1
HGS
SYT7
HPS1
DNASE2
OLFM4
MFSD8
LYN
LAMP3
STX3
STX7
CLN8
TOM1L1
SLC17A5
ABCA1
ZKSCAN4
AZU1
GATA2
relative
min
max
B
Mitochondria
mRNA rel. to control (Log)
HK2
MFN2
PPARGC1A
CLU
BCL2
MCU
A495V #72
G488R #12
G488R #22
C
Oxidative Stress
mRNA rel. to control (Log)
SOD2
SOD3
SESN3
CAT
TACR1
NRF2
GPX1
D
Lysosome
mRNA rel. to control (Log)
CTSF
GALC
HEXA
HPS1
LAMP3
TFEB
PLA2G3
LRRK2

Figure S4, related to Figure 1.

RNA-Seq analysis reveals different gene expression of gene involved in oxidative stress pathway.

(**A**) Heat-map of the unsupervised hierarchical clustering (UHC) of three different gene pathways related to mitochondria, oxidative stress and lysosomes. (**B-D**) qPCR analysis confirms the expression level difference for a selected number of genes between PD-OPA1 and ND NPCs. Quantification was normalized to ND NPCs. Data are mean ± SEM, n=3 independent experiments. *P<0.05, **P<0.01, ***P<0.001. Statistical analysis is performed by one-way ANOVA followed by Tukey post-test.

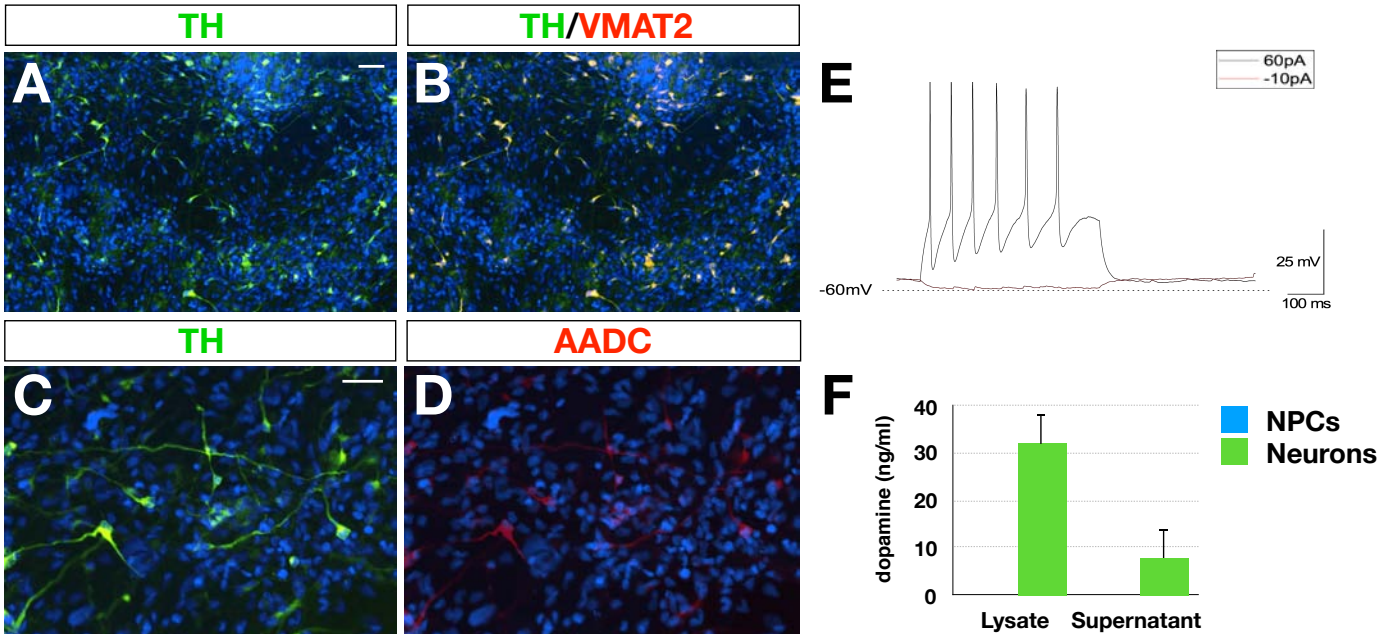
TH
TH/VMAT2
A
B
E
60pA
-10pA
25 mV
-60mV
100 ms
TH
AADC
C
D
F
dopamine (ng/ml)
40
30
20
10
0
NPCs
Neurons
Lysate
Supernatant

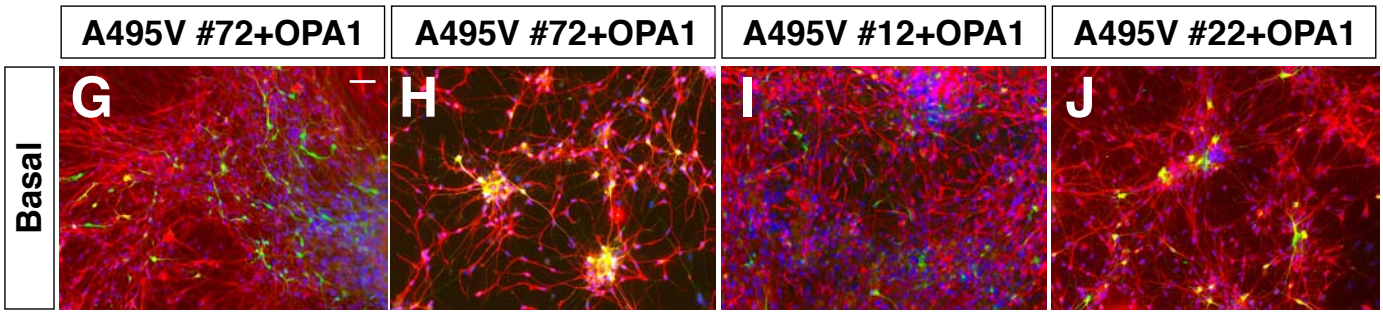
A495V #72+OPA1
A495V #72+OPA1
A495V #12+OPA1
A495V #22+OPA1
Basal
G
H
I
J

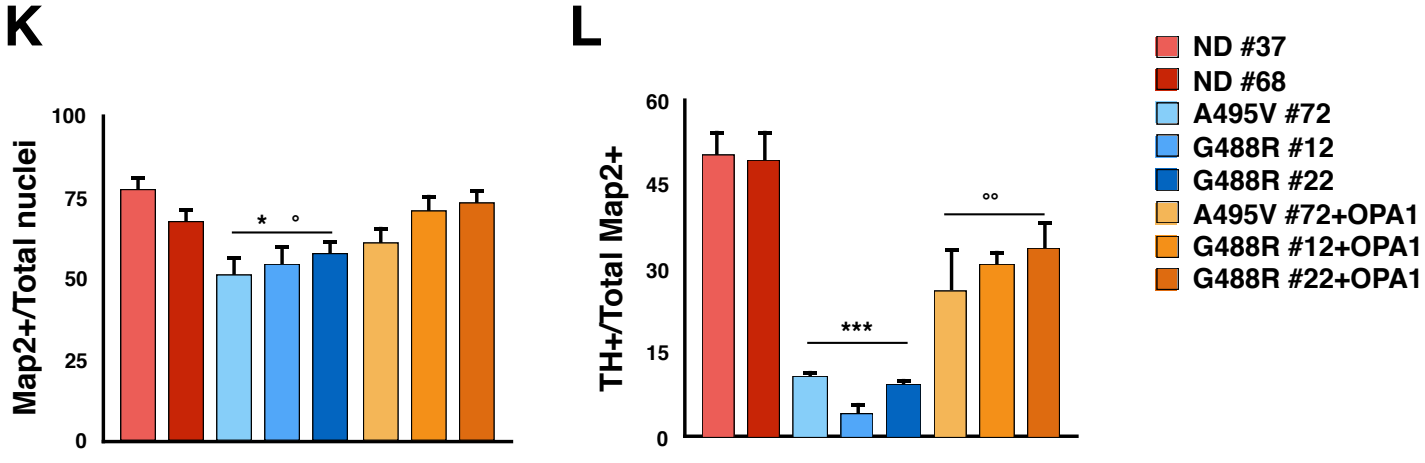
K
Map2+/Total nuclei
100
75
50
25
0
* °
L
TH+/Total Map2+
60
45
30
15
0
***
°°
ND #37
ND #68
A495V #72
G488R #12
G488R #22
A495V #72+OPA1
G488R #12+OPA1
G488R #22+OPA1

Figure S5, related to Figure 6.

Neuronal differentiation potential between ND and OPA1 gene reconstituted mutant NPCs is comparable.

(**A-D**) NPC-differentiated neuronal cultures include a sub-group of TH+ neurons co-expressing VMAT2 and AADC. (**E**) Current-clamp recording of multiple action potentials evoked by current injection in differentiated neurons. (**F**) Dopamine content measured by HPLC in NPCs and 2-months old neurons both in cell lysates and in supernatant after K+ stimulation. (**G-J**) TH (green) and MAP2 (red) immunofluorescence staining for OPA1 complemented and ND NPC-derived neurons in basal condition. (**K,L**) OPA1 gene complemented NPCs generate a comparable number of viable neurons compared to ND NPCs after two months in culture. Data are expressed as mean ± SEM of n=4 independent experiments. *P<0,05, ***P<0,001 to ND NPC-derived neurons and °P<0,05; °°<P0,01; °°°P<0,001 to OPA1 gene complemented NPC-derived neurons. Statistical analysis is performed using one-way ANOVA followed by Tukey post-test. Scale bars, 100 μm.

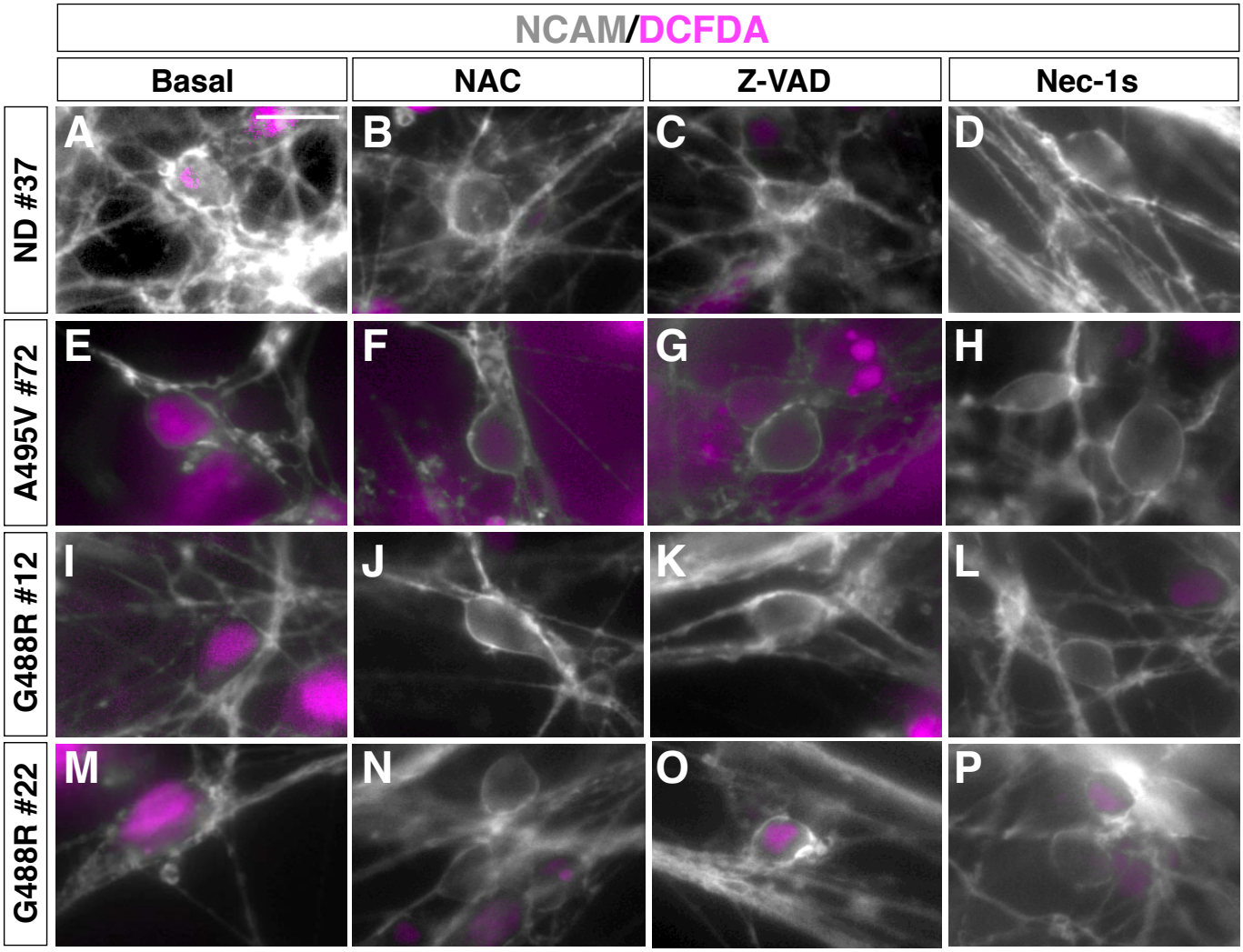
NCAM/DCFDA
Basal
NAC
Z-VAD
Nec-1s
ND #37
A495V #72
G488R #12
G488R #22
A
B
C
D
E
F
G
H
I
J
K
L
M
N
O
P

Q

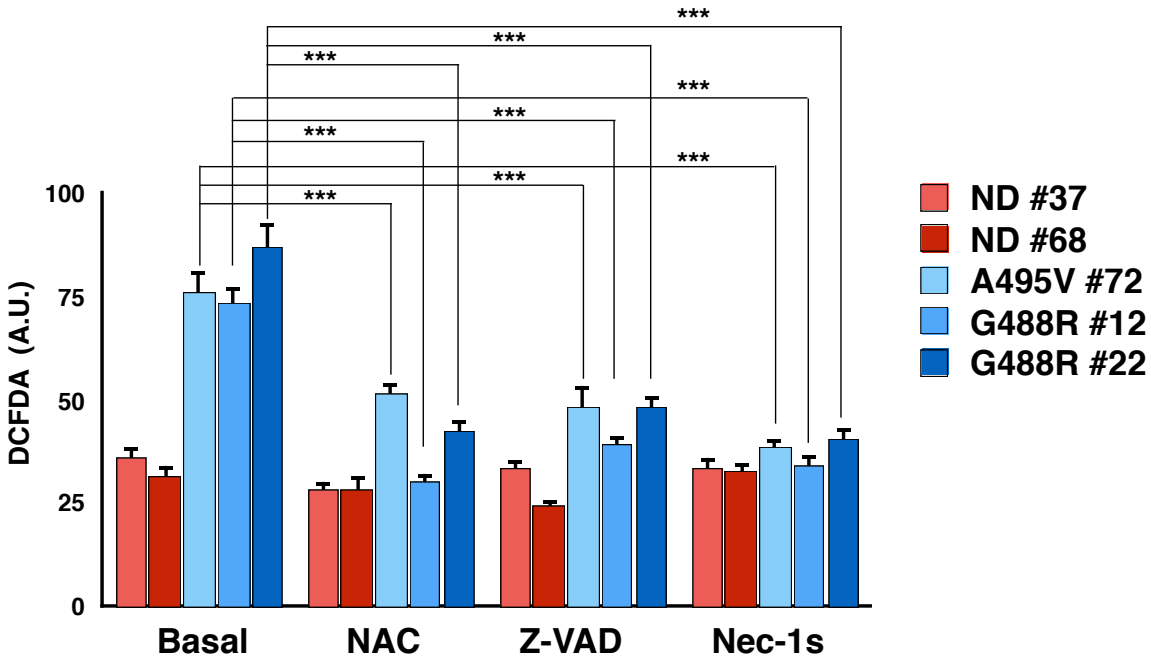
***
***
***
***
***
***
***
***
***
100
75
50
25
0
DCFDA (A.U.)
Basal
NAC
Z-VAD
Nec-1s
ND #37
ND #68
A495V #72
G488R #12
G488R #22

Figure S6, related to Figure 6.

PD OPA1 mutant NPC-derived neurons show an increased oxidative state.

(**A-P**) Representative images of neurons stained with the neuron-specific anti-NCAM antibody (gray) and the ROS-sensitive fluorescent probe DCFDA (purple) in basal condition and after NAC, Z-VAD and Nec-1s treatment. (**Q**) Quantification of DCF fluorescence signal indicates Nec-1s as the most effective treatment for reducing the oxidative stress in NPC-derived neurons. Values are mean ± SEM of n=4 independent experiments. ***P<0.001. Statistical analysis is performed using two-way ANOVA followed by Bonferroni post-test. Scale bars, 100 μm.

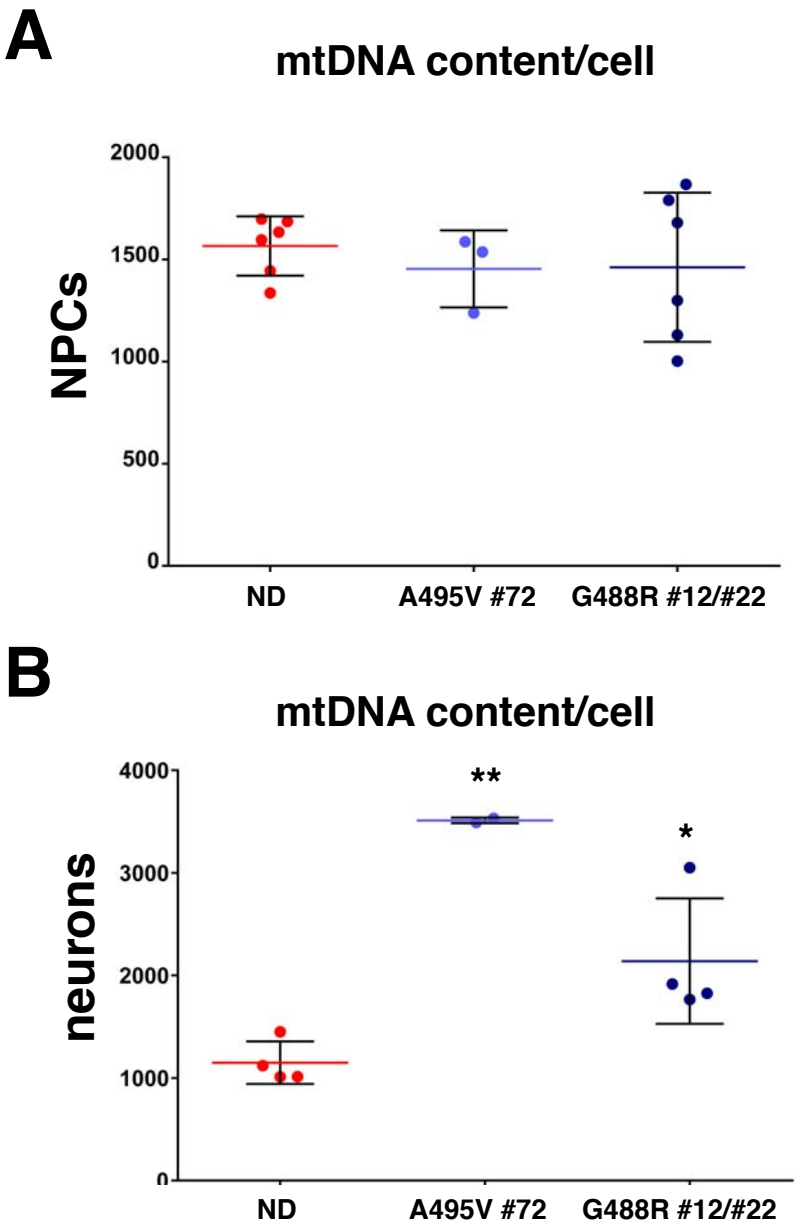

Figure S7, related to Figure 6.

Higher mtDNA copy number in PD OPA1 mutant NPC-derived neurons.

(**A**) Quantification of mitochondrial DNA (mtDNA) reveals comparable levels in PD-OPA1 and normal donor NPCs. (**B**) In contrast, PD-OPA1 compared to ND NPCs present a significant increase in the mtDNA copy number. Data expressed as mean ± SEM, n=3 independent experiments. *P<0,05; **P<0.01 Statistical analysis is performed using one-way ANOVA followed by Tukey post-test.

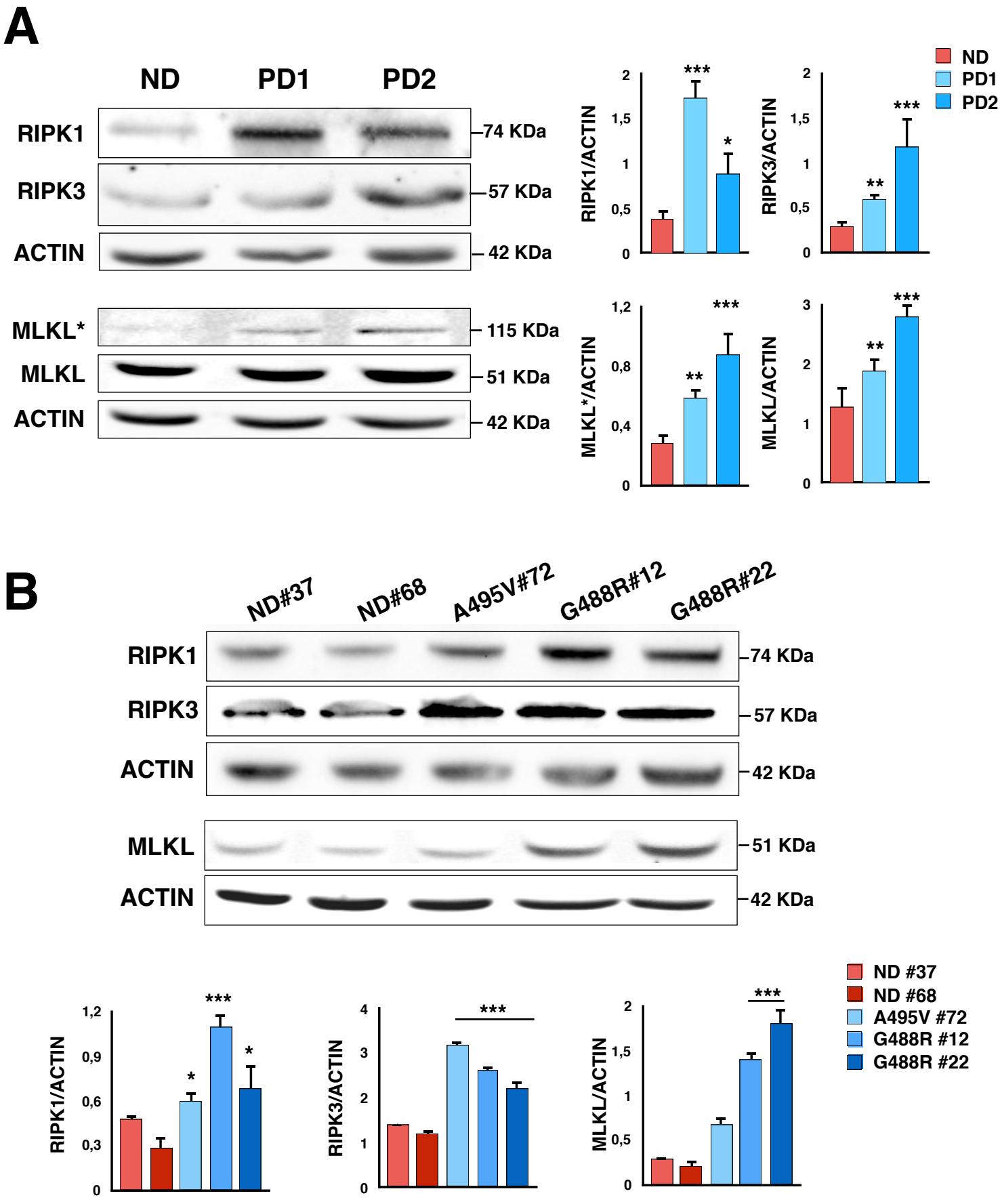
A
ND
PD1
PD2
RIPK1
RIPK3
ACTIN
74 KDa
57 KDa
42 KDa
MLKL*
MLKL
ACTIN
115 KDa
51 KDa
42 KDa
RIPK1/ACTIN
RIPK3/ACTIN
MLKL*/ACTIN
MLKL/ACTIN
ND
PD1
PD2
B
ND#37
ND#68
A495V#72
G488R#12
G488R#22
RIPK1
RIPK3
ACTIN
MLKL
ACTIN
74 KDa
57 KDa
42 KDa
51 KDa
42 KDa
RIPK1/ACTIN
RIPK3/ACTIN
MLKL/ACTIN
ND #37
ND #68
A495V #72
G488R #12
G488R #22

Figure S8, related to Figure 7.

RIPK1, RIPK3 and MLKL are upregulated in PD-OPA1 NPCs and in SN tissue from PD patients.

(A) Overall RIPK1, RIPK3 and MLKL protein levels are significantly increased in SN tissue lysates from PD patients respect to the normal donor (ND). MLKL*= protein dimers. **(B)** Western-blot analysis revealed the upregulation of the same necroptotic markers in PD-OPA1 compared to ND NPCs. *$p < 0.05$; ***$p < 0.001$ to ND Statistical analysis is performed using one-way ANOVA followed by Tukey post-test.

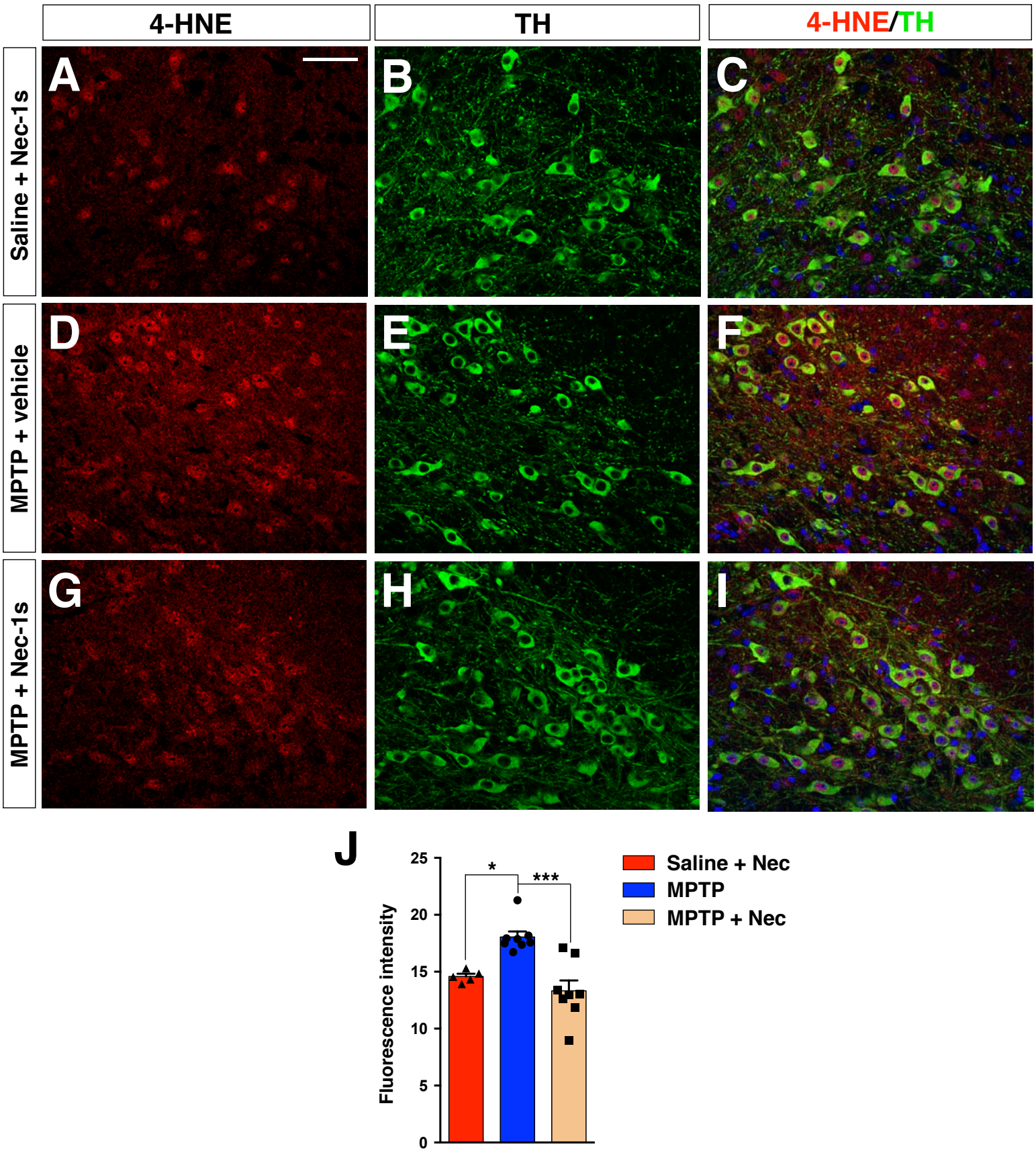
4-HNE
TH
4-HNE/TH
Saline + Nec-1s
MPTP + vehicle
MPTP + Nec-1s
A
B
C
D
E
F
G
H
I
J
Fluorescence intensity
25
20
15
10
5
0
*
***
Saline + Nec
MPTP
MPTP + Nec

Figure S9, related to Figure 7.

Nec-1s decreases ROS-mediated lipid oxidation in MPTP-treated mice.

(A-I) Representative pictures of 4-HNE staining (red) measured in TH positive (green) neurons. **(J)** Dopaminergic cells in MPTP-treated mice display an increase of lipid oxidation, which returns to basal levels in the presence of Nec-1s. The quantification is carried out measuring the levels of greys of 4-HNE staining in 8-bit images. Fluorescent images are captured as single layer. Values are means ± SEM for 5-8 mice (at least 10 cells are analyzed for each mouse). **$p < 0.01$; ***$p < 0.001$. Statistical analysis is performed using one-way ANOVA followed by Tukey post-test. Scale bar 60 μm.